Conformation of a water-soluble derivative of taxol in water by 2D-NMR spectroscopy

Luigi Gomez Paloma†, R Kiplin Guy, W Wrasidlo, KC Nicolaou*

Department of Chemistry, The Scripps Research Institute,10666 North Torrey Pines Road, La Jolla,CA 92037, USA
and Departments of Chemistry and Biochemistry, University of California, San Diego,
9500 Gilman Drive, La Jolla, CA 92093, USA

Background: Taxol is a natural product produced by the Pacific yew, *Taxus brevifolia*, that has emerged as a prominent chemotherapeutic agent for the treatment of solid tumors. It binds to microtubules, stabilizing them and arresting cells in mitosis. Taxol has been produced synthetically and a wealth of structure–activity data has recently emerged. To date, however, no single conformational model exists for the interpretation of these data. Studies of taxol and its analogs in organic solvents showed two distinct conformations, one in which the 3'-benzamido group and the 2-benzoyl group are in close proximity, and another in which the 2-benzoyl group is instead close to the 3'-phenyl group. We decided to use a derivative of taxol that has improved water-solubility to determine the structure of taxol in water.

Results: We have synthesized and characterized a stable water-soluble derivative of taxol that binds to microtubules and has a cytotoxicity profile very similar to that of taxol. 1D and 2D ^1H NMR experiments with this bioactive compound in D_2O indicate the presence of one conformer with a well-defined structure. In this structure, the 2-benzoyl group is clustered with the 3'-phenyl group.

Conclusion: The determination of the conformation of taxol in water may allow quantitative three-dimensional interpretation of the structure–activity data obtained for taxol, and hence enable the design of novel taxol mimics.

Chemistry & Biology October 1994, **1**:107–112
Key words: molecular design, solution NMR, taxol

Introduction

Taxol [1,2], originally isolated from *Taxus brevifolia* [3], is a newly approved anticancer agent used against breast and ovarian cancer that also has potential for the treatment of several other types of cancer [4]. Taxol acts by binding to microtubules; it both increases the rate of formation of microtubules from tubulin and stabilizes the resulting aggregates [5]. The microtubules in the mitotic spindle are particularly sensitive to the effects of taxol, as they assemble and disassemble unusually rapidly. Taxol therefore causes cells to arrest in their traverse through the cell cycle, predominantly at the G2/Prophase transition into mitosis. These arrested cells have an altered morphology, with stable bundles of microtubules and an abnormal mitotic spindle [6].

Although the structural nature of taxol's binding site is not known, taxol's affinity for its receptor seems to be high. As compounds with high binding affinities often [7], though not always [8], have the same conformation in solution as they do in the bound state, it is possible that knowledge of the conformation of taxol in aqueous solution could be used to design biological mimics of the drug. Such mimics might have improved binding properties for the taxol receptor on microtubules, and it might also be possible to use them to elucidate further the mode of action of the drug. Several NMR studies of the conformations of taxol (compound 1, Fig. 1) and its analog taxotere (compound 2, Fig. 1) have been carried out in organic solvents [9–14] and mixtures of DMSO: D_2O [15–17]. These studies have shown two predominant models for the solution structure of taxol. In one conformation, the 'apolar' model, the 3'-benzamido group and the 2-benzoyl group are in close proximity. In the other, called the 'hydrophobic collapse' model, the 3'-phenyl and 2-benzoyl groups are abutting one another. No consensus yet exists for the actual bioactive conformation of taxol.

We recently embarked on a program to develop a water-soluble prodrug of taxol by introducing a temporary polar or charged group into the taxol skeleton [18,19]. As the 7 position of taxol is known to tolerate substitution [1,2], a number of the derivatives prepared in this study were altered at this location. During these studies, the introduction of a methyl pyridinium moiety [20] was found to be a versatile way to add a temporary charge to organic molecules. The 7-methyl pyridinium salt of taxol, compound 3 (Fig. 1), emerged as a highly stable ($t_{1/2}$ > 30 d in H_2O) and highly soluble (> 10 mM in H_2O) derivative of taxol. Although this compound is not useful as a prodrug for taxol as a result of its high stability and rapid excretion *in vivo*, molecular dynamics and mechanics calculations (using MM2 force fields) with taxol and compound 3 indicated that the additional aryl ring of compound 3 should lie in a position that does not significantly perturb the conformation of the taxoid skeleton or that of the side chain. These properties led us to investigate the biological properties and structure in water of compound 3. In this paper we report the

*Corresponding author. †On leave from the University of Naples, Italy.

 ISSN 1074–5521

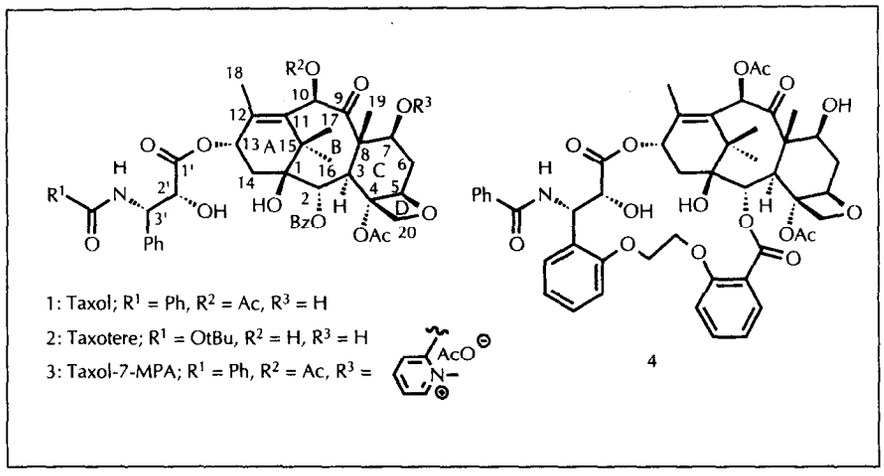

Fig. 1. Structures of taxol a i s ceriva-tives. The figure shows the t ct ires of taxol, compound 1; taxoter x m ound 2; the water-soluble tax d r vative taxol-7-MPA, compound 3 c tethered taxoid, compound 4.

synthesis of this water-soluble taxol, a 2D-NMR study of this bioactive taxol derivative, and a proposed conformational model for taxol in water.

Results and discussion

Chemical synthesis and biological activity

Compound 3 was synthesized in one step and good yield from commercially available taxol and 2-fluoro-1-methyl-pyridinium tosylate [20]. Like taxol, compound 3 stabilizes microtubules to calcium chloride-induced depolymerization (Fig. 2), indicating that this taxoid can still bind to the appropriate receptor, and that the binding regions are not significantly distorted from their conformation in taxol. Also, compound 3 exhibits a cytotoxicity profile very similar to that of taxol (Fig. 3) although slightly attenuated, presumably due to the fact that compound 3, being charged, is likely to have more difficulty in passively diffusing across the cellular membrane

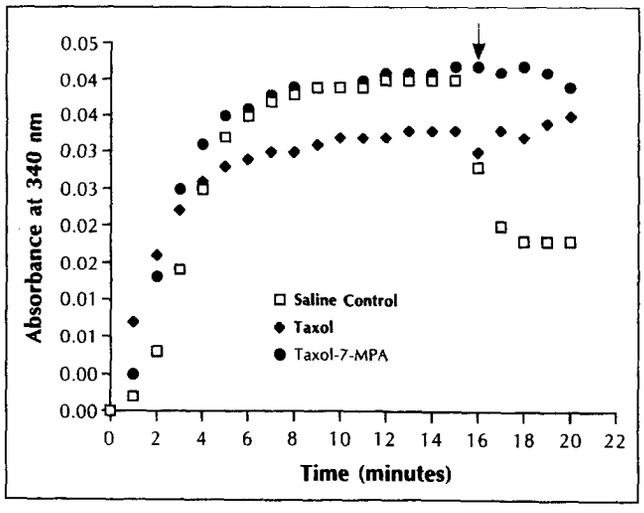

Fig. 2. Compound 3 has similar activity to taxol in tubulin polymerization–depolymerization experiments. Calcium chloride- promoted depolymerization is suppressed by taxol (compound 1, see Fig. 1) and taxol-7-MPA (compound 3). Calcium chloride addition is indicated by the arrow. Open squares, saline control; filled diamonds, taxol; filled circles, taxol-7-MPA (compound 3).

Table 1. Proton chemical shifts of compound 3 (500 MHz, D_2O) at 283 K*.

Position	δH
2	5.58 d (7.3)
3	3.81 d (7.3)
5	5.20 m
6α	2.91 m
6β	2.11 m
7	5.21 m
10	5.92 s
13	6.04 t (9.2)
14α	1.93 dd (14) 9.2)
14β	1.71 dd (14) 9.2)
16	1.02 s
17	1.10 s
18	1.69 s
19	1.91 s
20α	4.40 AB
20β	4.25 AB
2′	4.84 d (6.9
3′	5.43 d (6.9
4-OAc	2.38 s
10-OAc	2.06 s
3′-Ph	
o-	7.42 d†
m-	7.41 t
p-	7.21 m
3′-NHBz	
o-	7.72 d
m-	7.45 t
p-	7.54 t
2-BzO	
o-	8.02 d
m-	7.60 t
p--	7.71 t
7β-*O*-MePyr	
o-	8.40 d
m-	7.46 t
p-	8.40 t
m′-	7.46 d
Me	3.77 s

*Assignments obtained by double quantum filter correlation spectroscopy (2QF-COSY) and NOESY spectra. u pling constants are in parentheses and given in Hz. The c mical shifts are referenced to 3-(trimethylsilyl)-propionic-2, 3,3-d_4 acid, sodium salt, using the HOD resonance previou calibrated.
†Aromatic vicinal coupling constants are 7.7 ± Hz.

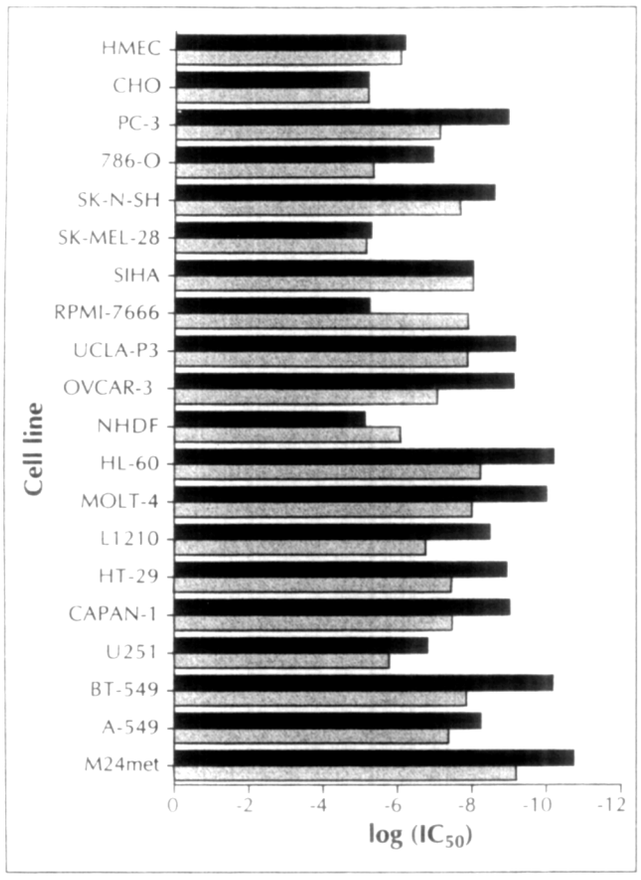

Fig. 3. Relative cytotoxicities of taxol and compound 3 for several cell lines. Compound 3 (taxol-7-MPA 3; shaded bars) exhibits cytotoxicities very similar to those of taxol (solid black bars). For cell lines used, see Materials and methods.

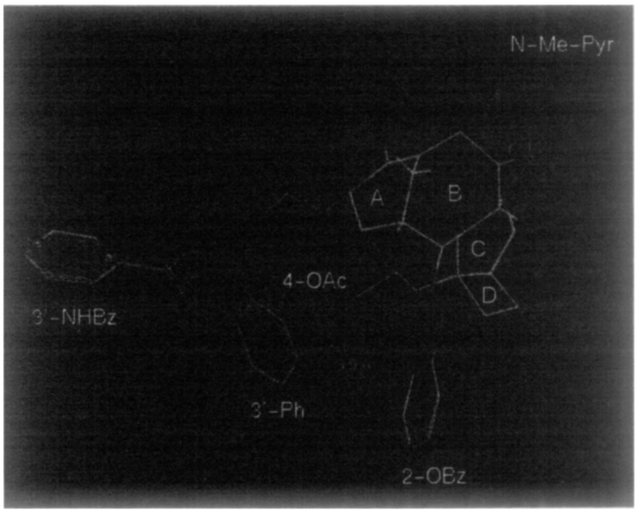

Fig. 4. NMR structure of compound 3. Superposition of 40 conformations of compound 3 obtained by refining different initial geometries using a combination of high temperature restrained molecular dynamics (1 000 K, 40 ps) and molecular mechanics calculations. The structures converged to a root-mean square deviation (RMSD) of 0.48 Å. This ensemble of conformations shows the high degree of structural organization of the side chains, most probably due to favorable interactions between the 2-benzoate, the 3'-phenyl, and the 4-acetyl groups. Hydrogens are omitted for clarity.

than taxol itself. Given these results, it was reasonable to expect that studies on the structure of compound 3 would reveal information about the aqueous conformation of taxol itself as well as, by inference, that of other biologically active taxoids.

NMR studies

Temperature-dependent 1D ^1H NMR (500 MHz, D_2O) experiments with compound 3 in D_2O revealed no significant changes in chemical shifts (< 0.05 ppm, Table 1) or coupling constants over the range of 274–344 K, suggesting one stable predominant conformation for compound 3. This observation is in accordance with the rigid nature of the polycyclic taxoid framework and strongly suggests organization of the side chain through special interactions.

The 2D NMR spectra of compound 3 recorded in D_2O (500 MHz, pH = 6.5, c = 1.0 mM) at 283 K led to a number of interesting observations and conclusions. Fig. 4 presents a superposition of 40 structures obtained by refining ten different initial geometries of compound 3 using restrained molecular dynamics (rMD) and mechanics calculations using NMR-derived constraints. Forty nuclear Overhauser effect measurements (NOEs) from two dimensional NOE spectroscopy (NOESY) spectra (500 MHz, τ_{mix} = 300 and 500 ms) were divided into strong, medium, and weak categories based on cross-peak volume measurements in both spectra (Table 2). A virtually identical pattern of dipolar effects is also observed in rotating-frame Overhauser effect spec-

Table 2. Selected NOEs observed in the NOESY spectra of compound 3 (500 MHz, D_2O, τ_{mix}=300 and 500 ms) at 283 K.

Proton 1	Proton 2	Strength*
o-H-BzO	*m*-H-Ph	m
m-H-BzO	*m*-H-Ph	m
o-H-BzO	H-20α	s
o-H-BzO	H-20β	s
o-H-BzO	H-14α	m
o-H-BzO	H-14β	m
o-H-Ph	H-14α	s
o-H-Ph	H-14β	s
Me_{17}	H-13	s
o-H-Ph	H-2′	w
o-H-Ph	H-3′	s
4-OCO*Me*	H-3′	m
4-OCO*Me*	*o*-H-BzO	s
4-OCO*Me*	*m*-H-Ph	m
4-OCO*Me*	H-2′	s
4-OCO*Me*	H-3	w
o-H-Pyr	H-7	m
o-H-Pyr	H-10	w
m-H-Pyr	H-7	s
m-H-Pyr	H-10	m
m-H-Pyr	H-6α	s
m-H-Pyr	H-3	w

*s = strong, m = medium and w = weak NOEs. This categorization is based on cross-peak volume measurements in both NOESY spectra (τ_{mix} = 300 and 500 ms).

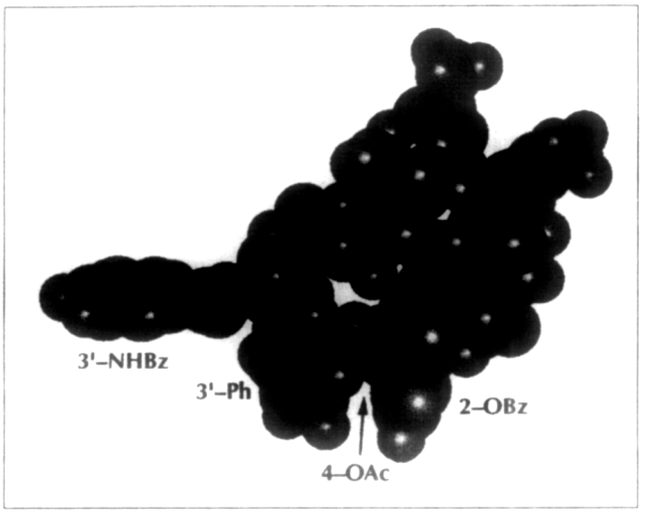

Fig. 5. Computer generated space-filling model of the closest structure to the mean conformation of compound 3. Atomic volumes presented in this model were obtained by scaling the van der Waals radii by 0.8. The atoms are displayed in color according to the following code: carbon, black; hydrogen, grey; oxygen, red; and nitrogen, blue.

troscopy (ROESY) under the same conditions. Upper bounds for the distance constraints were set at 2.7, 3.5 and 4.5 Å for strong, medium, and weak NOEs, respectively. All lower bounds were set at 1.8 Å. All the molecular dynamics and mechanics calculations were performed using the CVFF-91 force field contained in DISCOVER 2.9 software package (Biosym, San Diego, CA). As preliminary results indicated that the final conformation obtained in the presence of solvent (a water box of 15 Å radius) was not significantly different from that obtained *in vacuo*, no explicit solvent molecules were included in the calculations.

Overall, the structure is well-defined (all atoms are found between structures with a root-mean square deviation (RMSD) of 0.48 Å and show no constraint violations >0.2 Å) except for the 3'-benzamido ring for which no experimental constraints could be obtained. A control calculation was also performed without NMR-derived distance constraints to check the robustness of the structure calculation protocol in searching the conformational space of compound 3. In this case, the 40 final structures had an RMSD of 3.5 Å.

As expected, the conformation of the polycyclic taxoid skeleton is sharply defined (Figs 4 and 5). Taxol's polycyclic system from this NMR structure has the same conformation as that observed in the crystal structure of taxotere [21]. The A ring (see Fig. 1) has a boat conformation as indicated by the pattern of NOEs across the A and B rings (for instance, a diagnostic NOE is that between H_{13} and Me_{17}) and by the two coupling constants between H_{13} and $H_{14\alpha}$ (J = 9.2 Hz) and H_{13} and $H_{14\beta}$ (J = 6.0 Hz). The B ring is in a chair–boat conformation as supported by a strong NOE between H_7 and H_{10}. Indeed, in the chair–boat conformation, these two protons appear very close to each other (~ 2.5 Å from MM2 calculations), whereas in the chair–chair conformation they are considerably further apart (> 4 Å).

The most interesting feature of the structure, however, is the clustering of the hydrophobic 3'-phenyl, the 2-benzoate, and the 4-acetyl groups in D_2O solution. This definitively confirms that the hydrophobic clustering seen for both taxol (compound 1) and taxotere (compound 2) in 75 % DMSO: 25 % D_2O solution [13–15] is indeed seen in pure water. The relative orientation of the two aryl groups is defined by several NOEs between protons assigned to the two different aromatic rings (for example, *o*-H of the 2-benzoate and *m*-H of the 3'-phenyl rings) and between aromatic protons of these groups and the C-14 protons. In the refined structures, the closest atoms of these two groups (the *o*-C of the 2-benzoate and the *m*-C of the 3'-phenyl) are separated on average by 3.9 ± 0.2 Å. The two phenyl rings seem to lie in nearly parallel planes (with an interplanar angle of approximately 20°), an orientation that allows strong hydrophobic and π–π interactions and minimizes the accessible space for water molecules (Fig. 5). Such an orientation of two parallel aromatic rings with their centers offset and separated by 3.6–4.0 Å, has been postulated to be particularly favorable for π–π interactions [22]. Based upon the observation of strong NOEs between the methyl group of the C-4 acetyl and the 3'-phenyl and 2-benzoate aromatic protons, we conclude that the 4-acetyl group also contributes to this lipophilic clustering.

The major question remaining is whether the assumption that the aqueous conformation of taxol is also the

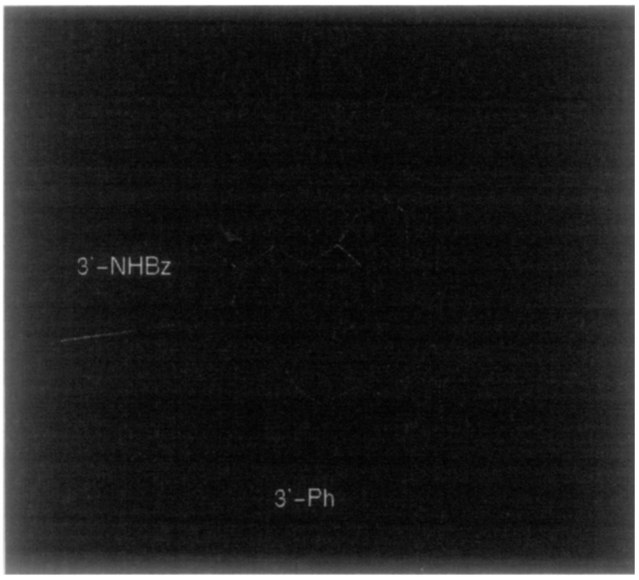

Fig. 6. Superposition of the NMR structure of taxol (compound 1, see Fig. 1) derived from the present study (green) and the energy minimized structure of the tether derivative compound 4 (white). The van der Waal's surface of taxol is displayed in blue. The areas of the molecule that are known to interfere with the binding to the receptor (from structure–activity relationship data [1]) are shown in yellow.

bioactive one is correct. To test this hypothesis, we have designed a conformationally locked derivative of taxol (compound 4, Fig. 1) which should reproduce the orientation of the 2-benzoate and 3'-phenyl groups found in the NMR structure of compound 3. For this purpose we investigated, by molecular modelling, the effect on the conformation of a number of tethers (consisting of three, four or five atoms) to connect and lock the 2-benzoate to the 3'-phenyl group. Several patterns of substitution on the two aromatic rings were analyzed. The structure–activity data for allowed substitutions on the aromatic rings were also included in the calculation [1]. On the basis of these computer modelling studies, an ethylene glycol tether linking the *meta* position of the 3'-phenyl to the *ortho* position of the 2-benzoate group was chosen as the best candidate. Fig. 6 shows a superposition of the determined NMR structure of taxol (compound 1) and this derivative (compound 4), in which the good alignment between the two molecules is quite clear. Compound 4 and related compounds are currently under construction in our laboratories.

Significance

Taxol seems likely to be an important weapon in the armory of anti-cancer drugs. The molecular basis of its action is unknown, however, hampering rational design of biological mimics with improved properties. An alternative approach is to start from a knowledge of the shape of the relevant form of taxol, and design small molecules that mimic that shape. One possibility is that the conformation of taxol in water is the relevant one for microtubule binding, and therefore for the cytotoxic and anticancer effects of taxol. Here we have firmly established the conformation of taxol in water.

The conformation of taxol in aqueous solution is tightly clustered as a result of hydrophobic interactions. The pharmacological significance of the hydrophobic clustering is still unknown, however, although experimental evidence suggests that all of the clustered groups are crucial elements for microtubule binding and activity *in vivo* [1,2]. We suggest that this hydrophobic cluster represents a preformed binding site for tight binding to tubulin. This hypothesis can be tested by designing molecules in which the hydrophobic cluster cannot change its conformation, and asking whether the effect of such compounds on microtubule stability is larger or smaller than that of natural taxol. These experiments are under way. If the hypothesis that the hydrophobic cluster is an important determinant of binding to microtubules proves correct, the detailed knowledge of the solution structure described here should be helpful in the design of novel taxol mimics.

Materials and methods

Chemical synthesis

Compound 3 was prepared from taxol (compound 1) by reaction with 2-fluoro-1-methylpyridinium tosylate (10 equiv) and triethylamine (40 equiv) in dichloromethane (0.05 M) at room temperature, followed by purification using reverse phase HPLC (Vydak RP-18 22.5 mm x 250 mm, 10 mM NH_4OAc in 20 % aq. MeOH→100 % MeOH over 30 min, 9 ml min^{-1}, UV; Rt (product) 26.6, (taxol) 28.7 min) to give compound 3 as an amorphous white solid (90 % average yield). The tosylate anion exchanges with an acetate ion during the HPLC purification procedure. Compound 3: mp 165–170 °(dec); $[\alpha]_D^{22}$ +9.5 (c = 1.0, $CHCl_3$); IR (neat) υ_{max} 2986, 1738, 1238, 1018 cm^{-1}; HRMS (FAB) obs 945.3825, calc for $C_{53}H_{57}O_{14}N_2$ 945.3810.

NMR experiments

All NMR experiments were performed on a Bruker AMX-500 using a sample of compound 3 in D_2O (c = 1.0 mM, pH = 6.5). The torsion angles for the side chain are as follows: C12–C13–O13–C1': −106 ± 2; C13–O13–C1'–C2': −156 ± 3; O13–/C1'–C2'–C3': 81 ± 2; C1'–C2'–C3'–CPh: −113 ± 3. The coordinates can be obtained through INTERNET by e-mail to rkg@scripps.edu or louis@scripps.edu. The 2D-NMR experiments were acquired and processed as described [21].

Structure calculations

The initial conformations were generated by randomizing torsion angles of the side chain and used in the subsequent rMD calculations (40 ps, 1000 K). Snapshots of the MD trajectory were taken every 10 ps. Each of these MD conformations was then subjected to restrained energy minimization, giving rise to 40 final refined structures. A harmonic penalty function was used for the NMR-derived constraints and the force constant was 32 kcal mol^{-1} $Å^{-2}$. The volume limits were established by a multiple calibration scheme, in which an effective calibration curve for the relationship between NOE volume and distance between protons is generated on the basis of the volumes for several different NOEs with distances that are fixed (for example, H20α/H20β and H-*ortho*/H-*meta* in aromatic rings).

Cytotoxicity measurements

Cells were harvested with trypsin/EDTA (Irvine Scientific), washed, resuspended in the appropriate medium, and counted in a hemocytometer using trypan blue. Cells were then plated on 96-well plates at 10^4 cells per well and incubated at 37 °C under 5 % CO_2 in sterile air, in a humidified incubator for 24 h. The drug was added directly to the wells from ethanol solutions across the range of 10^{-4} to 10^{-13} M. The final concentration of ethanol in the wells was 1 %. A solution of SDS (1 x 10^{-3} M) was used as the positive cytotoxicity control, and a well with no cells was used as the negative control. After incubation for 72 h, 50 µl of XTT (Polysciences, 2,3-*bis*(methoxy-4-nitro-5-sulfophenyl)-5[(phenyl-amino) carbonyl]-2H-tetrazolium hydroxide, 1 mg ml^{-1}) in phosphate-buffered saline (100 mM) was added to each well. In the presence of viable cells, this colorless pink solution is enzymatically transformed to give a pink coloration. The cytotoxicity was quantified by measuring the absorbance of the solution (OD) at 450 nm using a microplate reader (Molecular Devices Micropulse Reader). Percentage cytotoxicity was calculated using the formula: % cytotoxicity = [1 − (OD drug treated cells − OD growth control)] x 100. Cell lines used: HMEC (human mammary epithelial cells); CHO (Chinese hamster ovary); PC-3 (human prostate adenocarcinoma); 786-O (human primary renal cell adenocarcinoma); SK-N-SH (neuroblastoma,

metastatic to bone marrow); SK-MEL-28 (human malignant melanoma); SIHA (human squamous carcinoma); RPMI-7666 (human peripheral blood lymphoblast); UCLA-P3 (human lung adenocarcinoma); OVCAR-3 (human ovarian carcinoma); NHDF (normal human dermal fibroblast); HL-60 (human promyelocytic leukemia); MOLT-4 (human T-cell lymphocytic leukemia); L-1210 (murine lymphocytic leukemia); HT-29 (human colon adenocarcinoma); CAPAN-1 (human CNS carcinoma); U-251 (human CNS cancer); BT-549 (human breast ductal carcinoma); A-549 (human lung carcinoma); M-24met (human melanoma, metastatic to lung).

Tubulin polymerization assays

Experiments were performed in 96-well plates at 37 °C following the standard protocol [23]. In each case, 1.0 mM GTP was used to promote the initial polymerization of tubulin. Negative control: tubulin (1.0 mg ml^{-1}) alone, $CaCl_2$ (0.25 mM) added after 15 min; positive taxol control: tubulin (1.0 mg ml^{-1}) with taxol (10^{-6} M), $CaCl_2$ (0.25 mM) added after 15 min; taxol-7-MPA: tubulin (1.0 mg ml^{-1}) with taxol-7-MPA (10^{-6} M), $CaCl_2$ (0.25 mM) added after 15 min. Turbidity was measured as optical density at 340 nm using a microplate reader (Molecular Devices Thermomax).

Supplementary material available

Expanded regions of 2QF-COSY and NOESY spectra recorded in D_2O.

Acknowledgements: We thank Dr Gary Siuzdak for mass spectroscopic assistance. This work was financially supported by the National Institutes of Health, USA. L.G.P. is an Assistant Professor of the University of Naples, Italy. R.K.G. thanks the Office of Naval Research for a predoctoral fellowship.

References

1. Nicolaou, K.C., Dai, W.-M. & Guy, R.K. (1994). The chemistry and biology of taxol. *Angew Chem.* **33**, 15–44.
2. Kingston, D.G.I. (1993). The taxane diterpenoids. *Fortsch. Chem. Org. Natur.* **61**, 1–206.
3. Wani, M.C., Taylor, H.L., Wall, M.E., Coggan, P. & McPhail, A.T. (1971). Plant antitumor agents. VI. The isolation and structure of taxol, a novel antileukemic and antitumor agent from *Taxus brevifolia*. *J. Am. Chem. Soc.* **93**, 2325–2327.
4. Lavelle, F. (1993). Taxoids: a new class of antimitotic agents. *Curr. Opin. Invest. Drugs* **2**, 627–635.
5. Schifft, P.B., Fant, J. & Horwitz, S.B. (1979). Promotion of microtubule assembly *in vitro* by taxol. *Nature* **277**, 665–667.
6. Schifft, P.B. & Horwitz, S.B. (1980). Taxol-stabilized microtubules in mouse fibroblast cells. *Proc. Natl. Acad. Sci. USA* **7** 561–1565.
7. Gomez Paloma, L., Smith, J.A., Chazin, W.J. & colaou, K.C. (1994). The interaction of calicheamicin with dup DNA: role of the oligosaccharide domain and identification of ltiple binding modes. *J. Am. Chem. Soc.* **116**, 3697–3708.
8. Thériault, Y., *et al.* & Fesik, S.W. (1993) Solution ucture of the cyclosporin A/cyclosporin complex by NMR. *Natur* **61**, 88-91
9. Chmurny, G.N., Hilton, B.D., Brobst, S., Look, S.A. Vitherup, K.M. & Beutler, J.A. (1992). ^1H and ^{13}C NMR assignments or taxol, 7-epitaxol, and cephalomannine. *J. Nat. Prod. Lloydia* **55**, 414–423.
10. Falzone, C.J., Benesi, A.J. & Lecomze, T.J. (1992). Characterization of taxol in methylene chloride by NMR spectroscopy. *Tetrahedron Lett.* **33**, 1169–1172.
11. Baker, J.K. (1992). Nuclear overhauser effect spectroscopy (NOESY) and dihedral angle measurements in the determination of the conformation of taxol. *Spectrosc. Lett.* **25**, 31–48.
12. Hilton, B.D., Chmurny G.N. & Muschick, G.M. (1992). Taxol: quantitative internuclear proton–proton distances in $CDCl_3$ solution from NOE data: 2D NMR ROESY build-up rates at 500 MHz. *J. Nat. Prod. Lloydia* **55**, 1157–1161.
13. Dubois, J., *et al.*, & Beloeil, J.C. (1993). Conformation of taxotere and analogues determined by NMR spectroscopy and molecular modeling studies. *Tetrahedron* **49**, 6533–6544.
14. Cachau, R.E., *et al.*, & Erickson, J.W. (1994). Solution structure of taxol determined using a novel feedback scaling procedure for NOE-restrained molecular dynamics. *Super Comp. Appl. High Perform. Comp.* **8**, 24–34.
15. Williams, H. J., *et al.*, & Krauss, N. E. (1993). NMR and molecular modeling study of the conformations of taxol and of its side chain methyl ester in aqueous and non-aqueous solution. *Tetrahedron* **49**, 6545-6560.
16. Velde, D.G.V., Georg, G.I., Grunewald, G.L., Gunn, C.W. & Mitscher, L.A. (1993). 'Hydrophobic collapse' of taxol and taxotere solution conformations in mixtures of water and organic solvent. *J. Am. Chem. Soc.* **115**, 11650–11651.
17. Williams, H.J., *et al.*, & Krauss, N.E. (1994). NMR and molecular modeling study of active and inactive taxol analogues in aqueous and nonaqueous solution. *Can. J. Chem.* **72**, 252–260.
18. Nicolaou, K.C., Reimer, C., Kerr, M., Rideout, D. & Wrasidlo, W. (1993). Design, synthesis and biological activity of protaxols. *Nature* **364**, 464–466.
19. Nicolaou, K.C., Guy, R.K., Pitsinos, E.N. & Wrasidlo, W. (1994). A prodrug of taxol with self-assembling properties. *Angew. Chem.* **33**, 1581–1583.
20. Mukaiyama, T. (1979). New synthetic reactions based on the onium salts of aza-arenes. *Angew. Chem.* **18**, 707–745.
21. Guéritte-Voegelein, F., *et al.*, Pascard, C. (1990). Structure of a synthetic taxol precursor: N-*tert*-butoxycarbonyl-10-deacetyl-N-debenzoyl taxol. *Acta. Crystallogr. C* **46**, 781–784.
22. Hunter, C.A. & Sanders, J.K.M. (1990). The nature of π–π interactions. *J. Am. Chem. Soc.* **112**, 5525–5534.
23. Merlock, R.A. & Wrasidlo, W. (1994). Determination of microtubule assembly–disassembly kinetics on 96 well plates. *Anal. Biochem.*, in press.

Received: **19 Aug 1994**; revisions requested: **29 Aug 1994**; revisions received: **2 Sep 1994**. Accepted: **7 Sep 1994**.